Molecular Therapy
Oncolytics
Original Article

Circular RNA circRAB31 acts as a miR-885-5p sponge to suppress gastric cancer progression via the PTEN/PI3K/AKT pathway

Xianlong Liang,[1,5] Chuan Qin,[1,3,5] Gangfeng Yu,[2] Xiong Guo,[1] Anqi Cheng,[1] Han Zhang,[4] and Ziwei Wang[1]

[1]Department of Gastrointestinal Surgery, The First Affiliated Hospital of Chongqing Medical University, Chongqing 400010, PR China; [2]Institute of Life Sciences, Chongqing Medical University, Chongqing 400010, PR China; [3]Department of Gastrointestinal Surgery, Chongqing University Three Gorges Hospital, Chongqing 404000, PR China; [4]Department of Digestive Oncology, Chongqing University Three Gorges Hospital, Chongqing 404000, PR China

Emerging evidence indicated that circular RNAs (circRNAs) play essential roles in cancer progression. A large number of circRNAs have been reported to modulate cancer carcinogenesis. However, the underlying mechanisms by which circRNAs regulate gastric cancer remain largely unclear. By using circRNA microarray, we identified that circRAB31 may serve as a tumor suppressor. circRAB31 was downregulated in gastric cancer tissues and gastric cancer cell lines compared with normal tissues and a human gastric epithelial cell line (GES-1). Overexpression of circRAB31 suppressed gastric cancer proliferation and metastasis *in vitro* and *in vivo*, whereas silencing of circRAB31 had the opposite effects. Bioinformatic analysis as well as pull-down and luciferase assays revealed that circRAB31 exerted tumor-suppressive functions by binding directly to miR-885-5p. In addition, we demonstrated that circRAB31 could suppress PI3K/AKT signaling via the phosphatase and tensin homologue (PTEN)—a downstream target gene of miR-885-5p. In summary, our results demonstrated that circRAB31 could serve as a sponge of miR-885-5p to regulate gastric cancer cell proliferation, migration, and invasion by affecting the PTEN/PI3K/AKT signaling.

INTRODUCTION

Gastric cancer (GC) is one of the most prevalent malignant tumors globally, which is the fifth and the fourth most common cause of cancer morbidity and mortality, respectively, among all tumors.[1,2] Despite improvements in the diagnosis and treatment of GC, the incidence of GC and subsequent mortality in Asian countries, especially in East Asian countries, are increasing year by year.[2,3] Emerging evidence shows that genetic mutations, epigenetic alterations, and aberrant activation of oncogenic signaling are involved in gastric carcinogenesis.[4–6] Understanding the genetic mechanism critical for gastric carcinogenesis is fundamental and could be conducive to developing individual treatment strategies for patients with GC.

Circular RNA (circRNA) is a member of the noncoding RNAs, with a covalent closed-loop structure; it is considered as a by-product of back-splicing.[7,8] circRNA has been identified as a novel noncoding RNA that plays a crucial role in tumor initiation and development.[9] It has been shown that circRNA could serve as a sponge for microRNA (miRNA) or interact with RNA-binding proteins in a variety of diseases.[10–12] In addition, emerging studies have proven that a large number of circRNAs could be translated; so, they could modulate cancer progression.[13–16] It is now believed that circRNAs serve as promising biomarkers or potential therapeutic targets in multiple cancers.[17–19] However, previous work mainly focused on the functional studies of circRNAs in GC,[10,20,21] and the underlying mechanism by which circRNAs modulate GC has not yet been fully elucidated.

In our study, we performed circRNA microarray and identified abnormally expressed circRNAs between GC tissues and adjacent normal counterparts. We showed that one circRNA derived from exons 2, 3, 4, and 5 of the Ras-related protein Rab-31 (RAB31) gene (termed circRAB31) was downregulated in tumor tissues and GC cell lines. circRAB31 was able to inhibit the proliferation, migration, and invasion of GC both *in vitro* and *in vivo*. Furthermore, we demonstrated that circRAB31 could serve as a sponge for miR-885-5p to modulate the phosphatase and tensin homologue (PTEN) expression, resulting in inhibition of the PI3K/AKT pathway. The circRAB31/miR-885-5p/PTEN/PI3K/AKT regulatory axis may offer novel therapeutic targets for patients with GC.

RESULTS

Characterization of circRAB31 and expression of circRAB31 in GC cells and tissues

We previously identified 5,508 dysregulated circRNAs in five GC tissues and compared adjacent normal tissues.[22] Then, we screened 215 differentially expression genes meeting the criteria of $p < 0.005$

Received 30 June 2021; accepted 8 November 2021;
https://doi.org/10.1016/j.omto.2021.11.002.

[5]These authors contributed equally

Correspondence: Ziwei Wang, MD, PhD, Department of Gastrointestinal Surgery, The First Affiliated Hospital of Chongqing Medical University, Chongqing 400010, PR China.
E-mail: wangziwei@hospital.cqmu.edu.cn

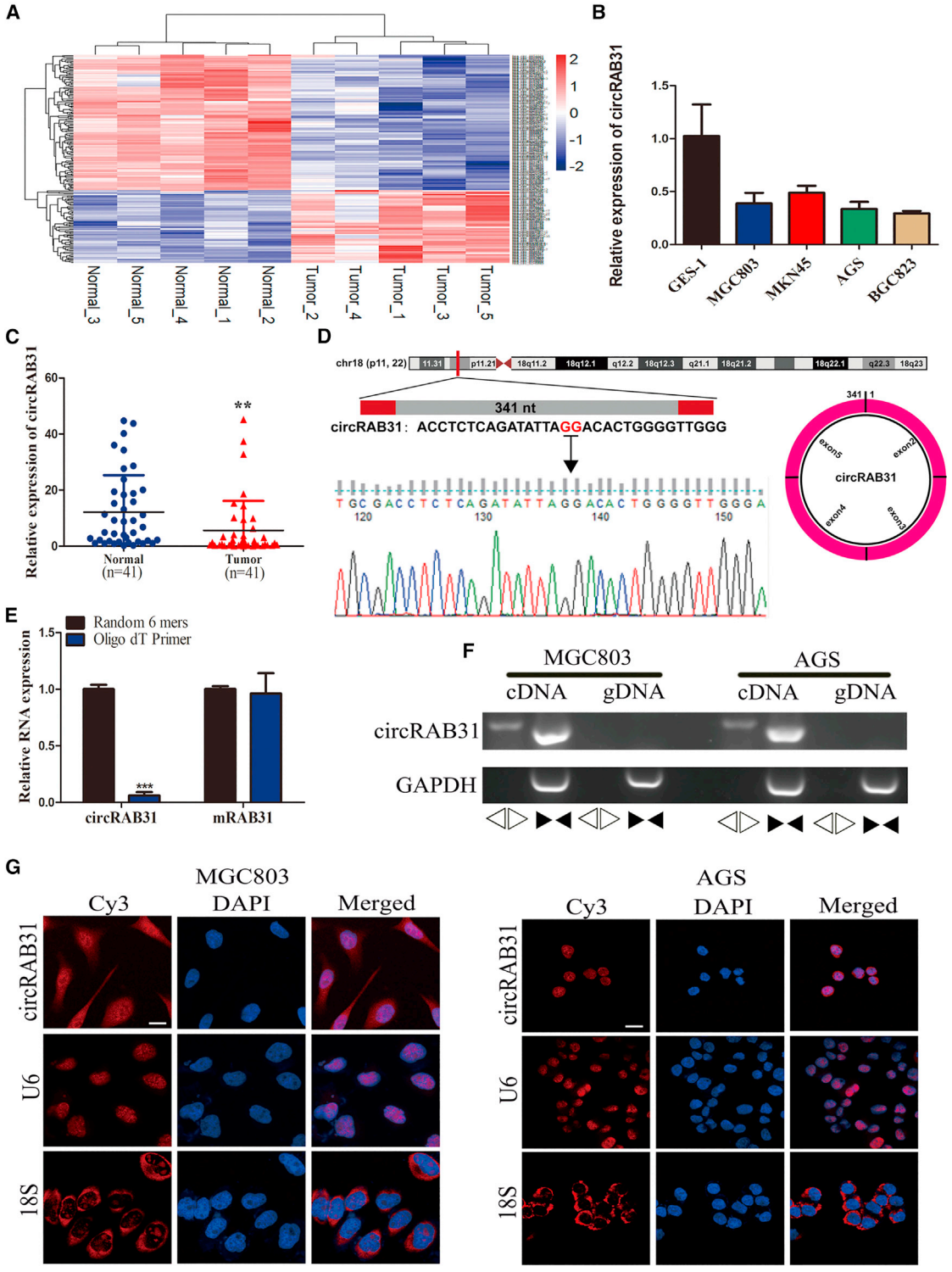

Figure 1. Characterization of circRAB31 and expression of circRAB31 in GC cells and tissues

(A) Heatmap of 215 differentially expressed circRNAs with $p < 0.005$ and expression peak >10,000. (B) Expression of circRAB31 in GC cell lines and GSE-1 cells. (C) circRAB31 was downregulated in 41 GC tissues compared with adjacent normal tissues (**$p < 0.01$). (D) We revealed the head-to-tail splicing of circRAB31 by Sanger

(legend continued on next page)

Table 1. Correlations between circRAB31 expression and clinicopathologic characteristics in GC patients

Characteristic	circRAB31			
	All (n = 41)	High (%) n = 12	Low (%) n = 29	p value
Gender				
Male	32	8 (25.0)	24 (75.0)	0.257
Female	9	4 (44.4)	5 (55.6)	
Age (years)				
>60	16	3 (18.7)	13 (81.3)	0.236
≤60	25	9 (36.0)	16 (64.0)	
Differentiation grade				
Good	11	4 (36.4)	7 (63.6)	0.545
Poor	30	8 (26.7)	22 (73.3)	
Tumor size				
≥50 mm	17	2 (11.8)	15 (88.2)	0.038[a]
<50 mm	24	10 (41.7)	14 (58.3)	
Lymph node				
N0	18	2 (11.1)	16 (88.9)	0.024[a]
N1-N3	23	10 (43.5)	13 (56.5)	
Stages				
I-II	22	10 (45.5)	12 (54.5)	0.014[a]
III-IV	19	2 (10.5)	17 (89.5)	

[a]$p < 0.05$.

and expression peak >10,000. Among the 215 dysregulated circRNAs, 74 (34.4%) were upregulated and 141 (65.6%) were downregulated in GC tissues compared with the adjacent normal tissues (Figure 1A). Among these circRNAs, hsa_circ_0008821 (termed as circRAB31) was the most significantly downregulated. To further validate whether circRAB31 was dysregulated in GC cells and GC tumors according to our microarray expression profile, we performed quantitative real-time PCR (qRT-PCR) and confirmed that circRAB31 was downregulated in MGC803, MNK45, AGS, BGC823 GC cell lines, and in 41 GC tumor tissues relative to a human gastric epithelial cell line (GES-1) and 41 paired adjacent normal tissues (Figures 1B and 1C). We also investigated the relationship between circRAB31 expression level and clinical features of GC patients. All patients were divided into two groups according to circRAB31 expression level: circRAB31 low group (n = 29, 70.7%) and circRAB31 high group (n = 12, 29.3%). The level of circRAB31 did not exhibit significant correlation with gender, age, and differentiation grade; however, its expression level was strongly correlated with tumor size, tumor stage, and lymph node metastasis of GC patients (Table 1). Survival analysis also indicated that patients in the circRAB31 high group have a better survival outcome than those in the circRAB31 low group (Figure S1A), which suggests low expression of circRAB31 is highly associated with GC malignancy.

circRAB31 (located at chromosome 18: 9,775,274–9,815,219) is derived from exon 2, exon 3, exon 4, and exon 5 of its parental gene, RAB31, a small guanosine 5′-triphosphate-binding protein (Figures 1D and S1B). By using sanger sequencing, we verified that circRAB31 was the product of back-splicing (Figure 1D). To further validate the characteristics of circRAB31, we performed qRT-PCR experiments by using random-hexamer or oligo (dT) 18 primers. Compared with the oligo (dT)-18-primers group, the relative expression of circRAB31 was significantly higher in the random-hexamer group (Figure 1E). We also confirmed that circRAB31 could be amplified using divergent primers from cDNA of GC cell lines but not from gDNA (Figure 1F). Besides, we conducted RNase R experiments and observed that the level of mRAB31 obviously reduced after treatment with RNase R, but RNase R could not affect RNA level of circRAB31 (Figure S1C), indicating that circRAB31 possesses a closed-loop structure. RNA fluorescence *in situ* hybridization (FISH) and qRT-PCR analysis after subcellular fractionation revealed the cytoplasmic and nuclear enrichment and localization of circRAB31 in MGC803 and AGS cells (Figures 1G, S1D, and S1E). These findings indicated that circRAB31 was downregulated in GC cell lines and tissues.

circRAB31 silencing promotes GC cell proliferation, migration, and invasion

To explore the function of circRAB31 in tumorigenesis and progression, we designed three small interfering RNAs (siRNAs) targeting circRAB31. Among those three siRNAs, si1 and si3 significantly inhibited the expression of circRAB31 in both MGC803 and AGS cells (Figure 2A). Considering circRAB31 and mRAB31 share part of the same sequences that might be targeted by siRNA of circRAB31, we determined the expression of mRAB31 in siRNA transfected GC cells targeting circRAB31. Results demonstrated that the expression of mRAB31 could not be affected by using siRNAs (Figure S1F), which indicated that two siRNAs (si1 and si3) are specifically targeting circRAB31. The Cell Counting Kit-8 (CCK-8) and colony formation assays revealed that silencing of circRAB31 promoted the proliferation ability of MGC803 and AGS cells. Meanwhile, 5-ethynyl-20-deoxyuridine (EdU) results indicated that silencing of circRAB31 promoted GC cell DNA synthesis ability (Figures 2B–2G). Then, we determined the function of circRAB31 in migration and invasion, that is, the silencing of circRAB31 significantly promoted the migration and invasion capabilities of MGC803 and AGS cells (Figures 2H–2K). Moreover, the wound-healing assay also indicated that the cell migration ability of MGC803 and AGS cells was enhanced by circRAB31 knockdown (Figures 2L–2M). We also detected the function of circRAB31 on cell apoptosis. However, results demonstrated that silencing of circRAB31 has no effect on apoptosis of GC cells (Figures S2A and S2B).

sequencing and demonstrated its genomic size as reported in the CircBase database. (E) We detected the expression levels of circRAB31 and mRNA of RAB31 in GC cells with oligo dT primer and random 6 mers (***$p < 0.001$). (F) By using divergent and convergent primers, PCR assay was performed to detect the expression of circRAB31 in cDNA or genomic DNA (gDNA) of GC cell lines. (G) FISH analysis indicated cytoplasmic and nuclear enrichment and localization of circRAB31 in GC cells; scale bar, 20 μm.

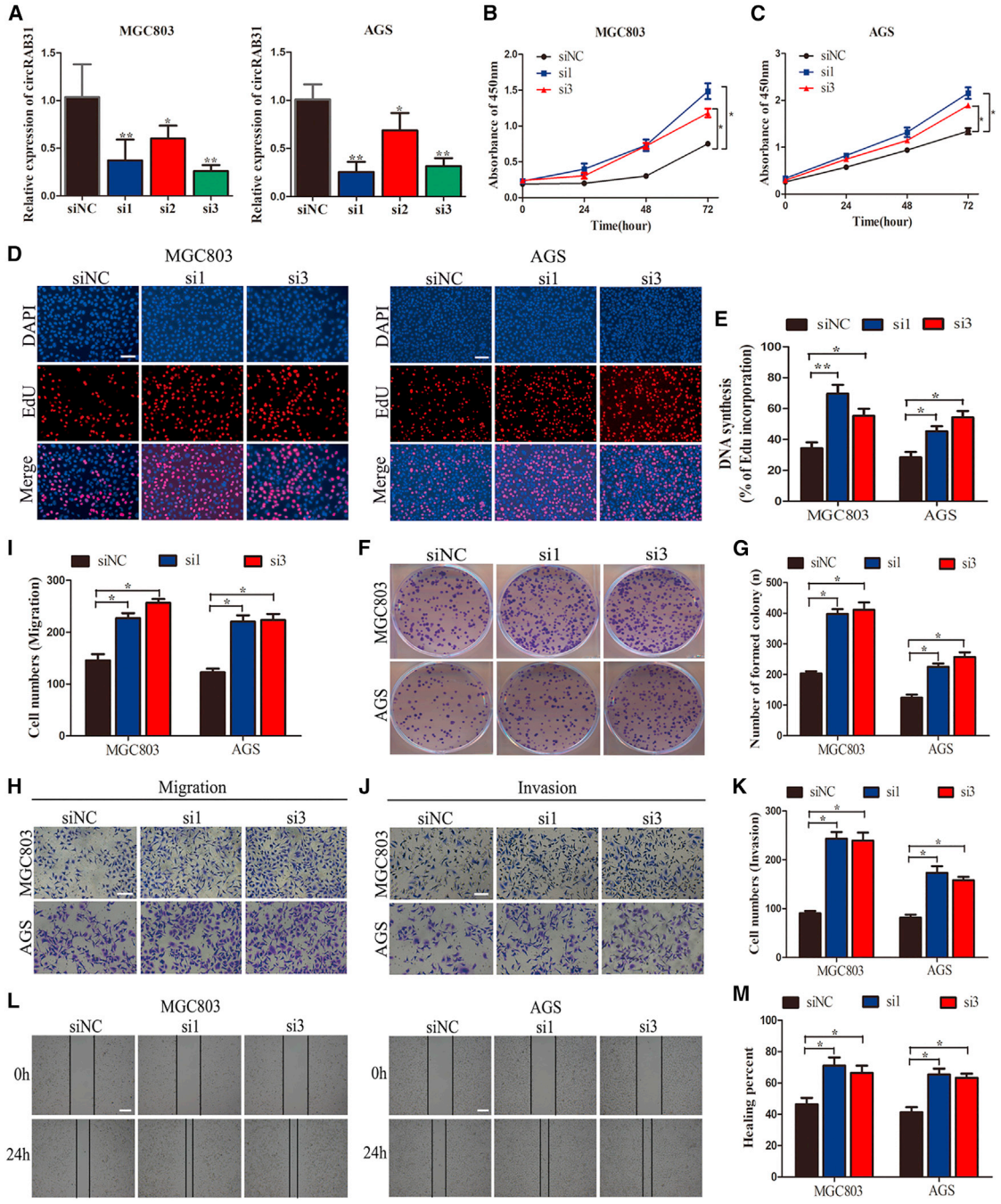

Figure 2. circRAB31 silencing promotes GC cell proliferation, migration, and invasion

(A) qRT-PCR experiment was performed to confirm the relative expression of circRAB31 in MGC803 and AGS cell lines after transfecting with three siRNAs targeting circRAB31 (*$p < 0.05$, **$p < 0.01$). (B–G) CCK-8, EdU, and colony formation assays were used to determine the proliferation of MGC803 and AGS cells after circRAB31 silencing; scale bar, 100 μm (*$p < 0.05$, **$p < 0.01$). (H–K) Transwell migration and transwell invasion assays illustrated that silencing of circRAB31 promote the migration and invasion abilities of GC cells; scale bar, 100 μm (*$p < 0.05$). (L and M) Wound-healing assay indicated that silencing of circRAB31 promotes the migration ability of GC cells; scale bar, 120 μm (*$p < 0.05$).

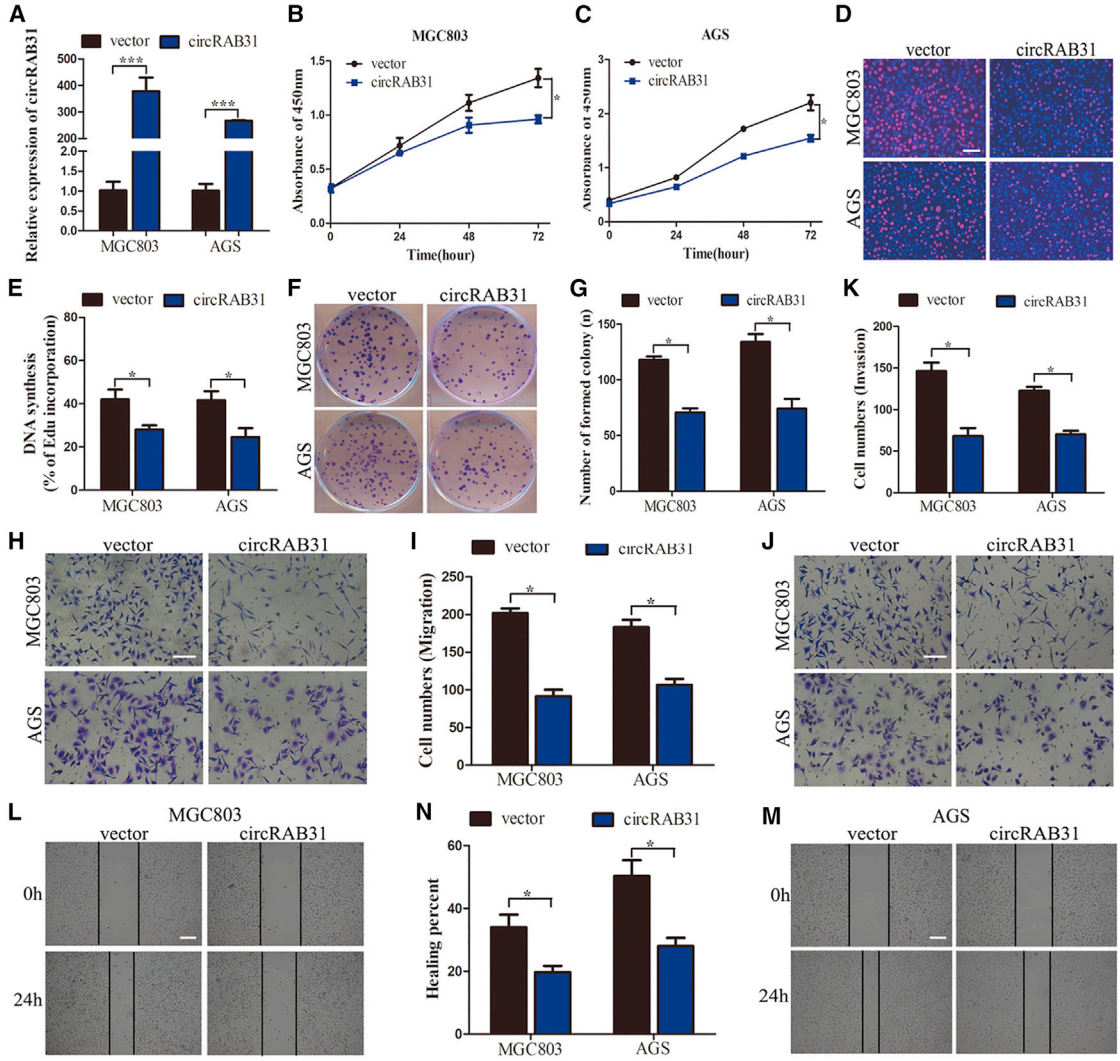

Figure 3. Overexpression of circRAB31 inhibits GC cell proliferation, migration, and invasion

(A) qRT-PCR was performed to confirm the overexpression efficiency of circRAB31 in MGC803 and AGS cells (***$p < 0.001$). (B–G) CCK-8, EdU, and colony formation assays indicated that overexpression of circRAB31 inhibits the proliferation ability of GC cells; scale bar, 100 μm (*$p < 0.05$). (H–K) Transwell migration and transwell invasion assays indicated that overexpression of circRAB31 significantly inhibits the migration and invasion abilities of GC cells (*$p < 0.05$). (L–N) Wound-healing assay indicated that overexpression of circRAB31 inhibits the migration ability of GC cells; scale bar, 120 μm (*$p < 0.05$).

Based on the downregulation of circRAB31 in GC tissues and cell lines, we further explored its functional role by overexpressing circRAB31 in MGC803 and AGS cell lines. Quantitative real-time PCR was used to validate the overexpression efficiency of circRAB31 (Figure 3A). Subsequently, CCK8, colony formation, and EdU assays were performed to detect the proliferation ability of MGC803 and AGS cells. Transwell migration and wound-healing assays were used to assess the migration ability of GC cells, and the invasion ability of GC cells was analyzed using transwell invasion assay. As expected, we observed that the overexpression of circRAB31 inhibited the cell proliferation rate, as determined by the CCK8 assay (Figures 3B and 3C); it also inhibited the colony formation ability and DNA synthesis, as indicated by the EdU assay (Figures 3D and 3G). In addition, overexpression of circRAB31 strikingly suppressed the migration and invasion abilities of MGC803 and AGS cell lines (Figures 3H–3N).

Taken together, the results of these *in vitro* experiments indicated that circRAB31 exerted tumor suppressor function in GC progression.

circRAB31 may serve as a sponge for miR-885-5p

Considering that mounting evidence has shown that circRNAs are involved in tumor development and progression as an miRNA sponge,[23,24] we proposed that circRAB31 could also function as an

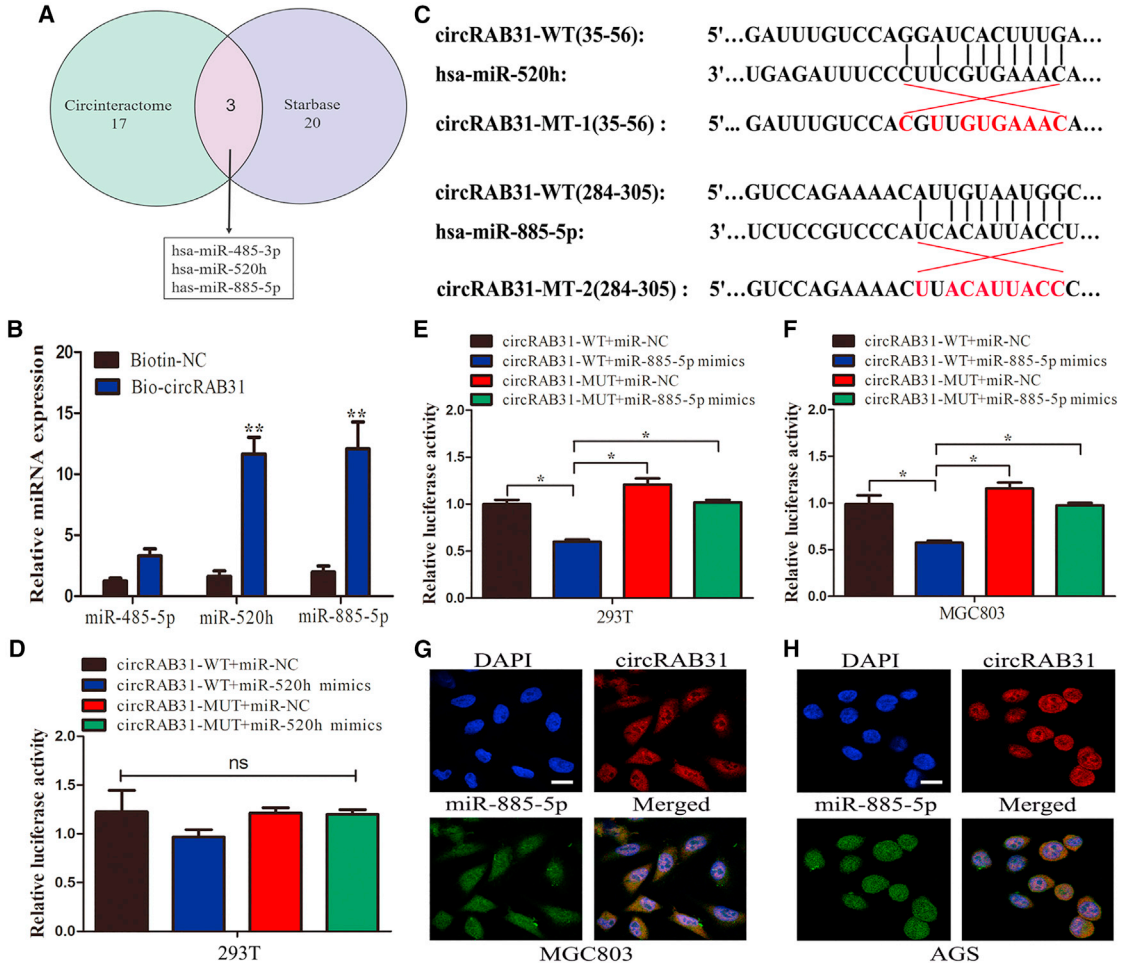

Figure 4. circRAB31 may serve as a sponge for miR-885-5p

(A) Circinteractome and Starbase online tools were used to predict target miRNAs of circRAB31. (B) Pull-down assay was performed to determine the direct binding between circRAB31 and three potential target miRNAs (**$p < 0.01$). (C) A schematic drawing exhibited that the putative binding sites of miR-520h and miR-885-5p with circRAB31. (D–F) The luciferase activity of pmirGLO-circRAB31-WT or pmirGLO-circRAB31-MUT in 293T cells and MGC803 cells after co-transfection with miR-520h or miR-885-5p (*$p < 0.05$). (G and H) Co-localization between miR-885-5p and circRAB31 was observed by RNA *in situ* hybridization in GC cells. Nuclei were stained with DAPI; scale bar, 20 μm.

miRNA sponge in GC tumorigenesis. To determine that, we predicted the potential targets of circRAB31 by cross-analyzing two prediction databases: Circinteractome and Starbase. Three miRNAs with putative binding sites for circRAB31 were identified (Figure 4A). Then, pull-down assay was performed to further determine the potential interaction between circRAB31 and three miRNAs. Compared with miR-485-5p, we observed that miR-520h and miR-855-5p were enriched by a specific biotin-labeled circRAB31 probe (Figure 4B). To further validate our findings, we constructed the full-length sequences of circRAB31-wild-type (WT) and circRAB31-mutant (MUT) without the luciferase vector of miR-520h or miR-885-5p binding sites (Figure 4C). In luciferase reporter assay, we observed that co-transfection of miR-885-5p mimics and circRAB31 resulted in a significant reduction of luciferase activity, while other groups did not induce obvious reduction in the luciferase activity (Figures 4D–4F and S2C). FISH assay was conducted to detect the localization of miR-885-5p and circRAB31 and showed that miR885-5p and circRAB31 were co-localized both in the nucleus and in the cytoplasm of GC cell lines (Figures 4G and 4H). In addition, we detected the correlation between expression level of circRAB31 and miR-885-5p. Interestingly, we observed that there was no significant correlation between circRAB31 and miR-885-5p (Figure S2D), indicating that although circRAB31 and miR-885-5p are combined, it will not affect the expression level of each other. These findings indicated the direct interaction between miR885-5p and circRAB31.

circRAB31 attenuated the ability of miR-885-5p to promote GC cell proliferation, migration, invasion

miR-885-5p has been shown to regulate the biological function of multiple cancer cells, including gastric cancer cells.[25–27] However, it remains unclear whether miR-885-5p is responsible for the ability of circRAB31 to inhibit GC cell proliferation, migration, and

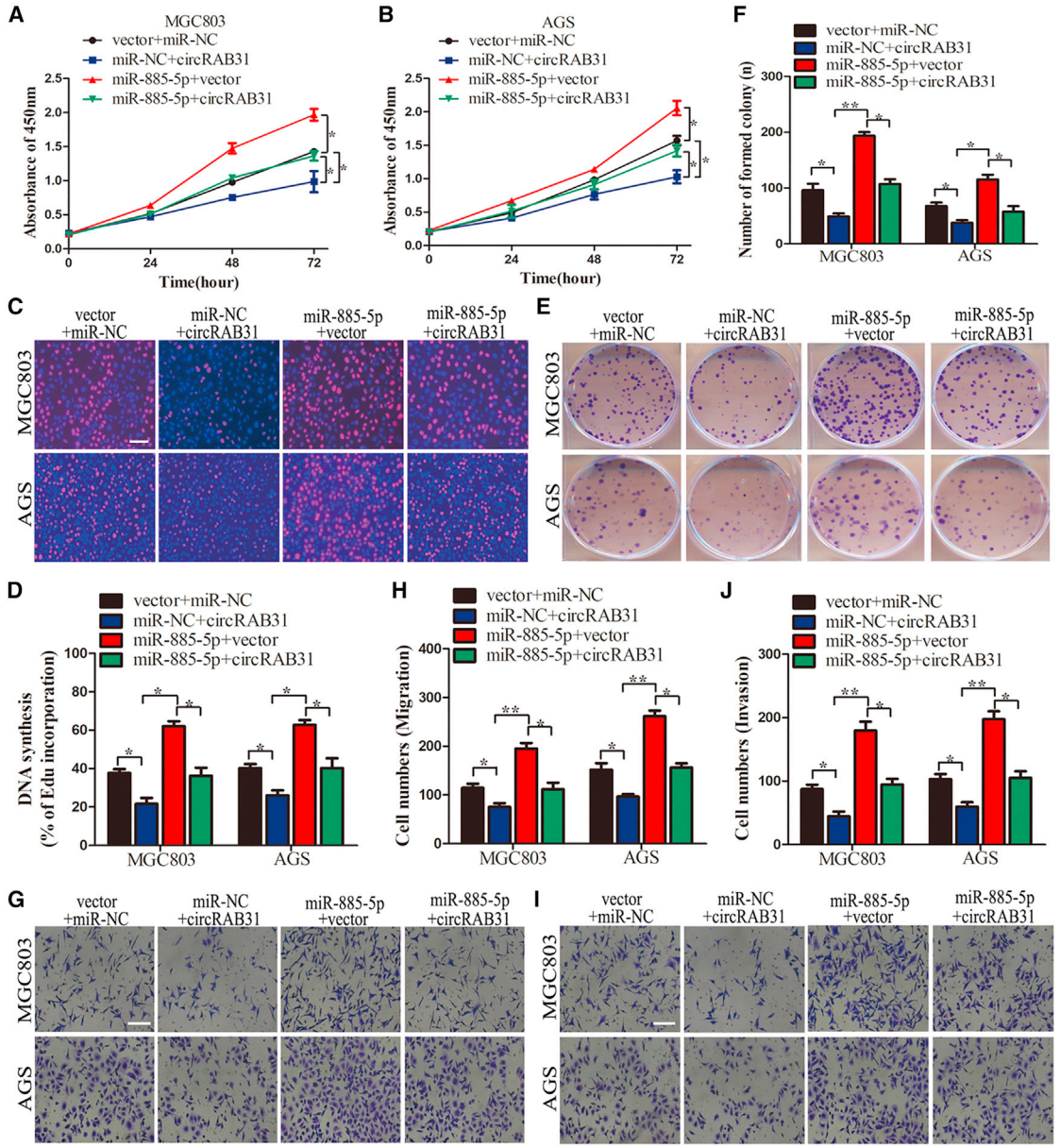

Figure 5. circRAB31 attenuated the ability of miR-885-5p in promoting GC cell proliferation, migration, invasion

(A–F) CCK-8, colony formation, and EdU assays illustrated that miR-885-5p mimics promote the proliferation ability of GC cells, while co-transfection with circRAB31 could attenuate the proliferation ability achieved by miR-885-5p; scale bar, 100 μm (*$p < 0.05$, **$p < 0.01$). (G–J) Transwell migration and transwell invasion assays were performed to detect the migration ability and invasion ability of MGC803 and AGS cells after the co-transfection of miR-885-5p mimics and circRAB31; scale bar, 100 μm (*$p < 0.05$, **$p < 0.01$).

invasion. Therefore, we performed rescue experiments to detect their correlation. In CCK-8 and colony formation assays, overexpression of circRAB31 was able to partially reverse cell proliferation and colony formation abilities induced by miR-885-5p mimics. Meanwhile, circRAB31 overexpression attenuated the DNA synthesis ability inhibition caused by miR-885-5p mimics in GC cells (Figures 5A–5F). Transwell migration assay showed that overexpression of circRAB31 partially weakened the increase in migration ability induced by miR-885-5p mimics (Figures 5G and 5H). In addition, transwell invasion assay demonstrated that circRAB31 overexpression partially attenuated the invasion ability favored by miR-885-5p mimics (Figures 5I and 5J). These results indicated that circRAB31 serves as a tumor suppressor by impairing the oncogenic function of miR-885-5p.

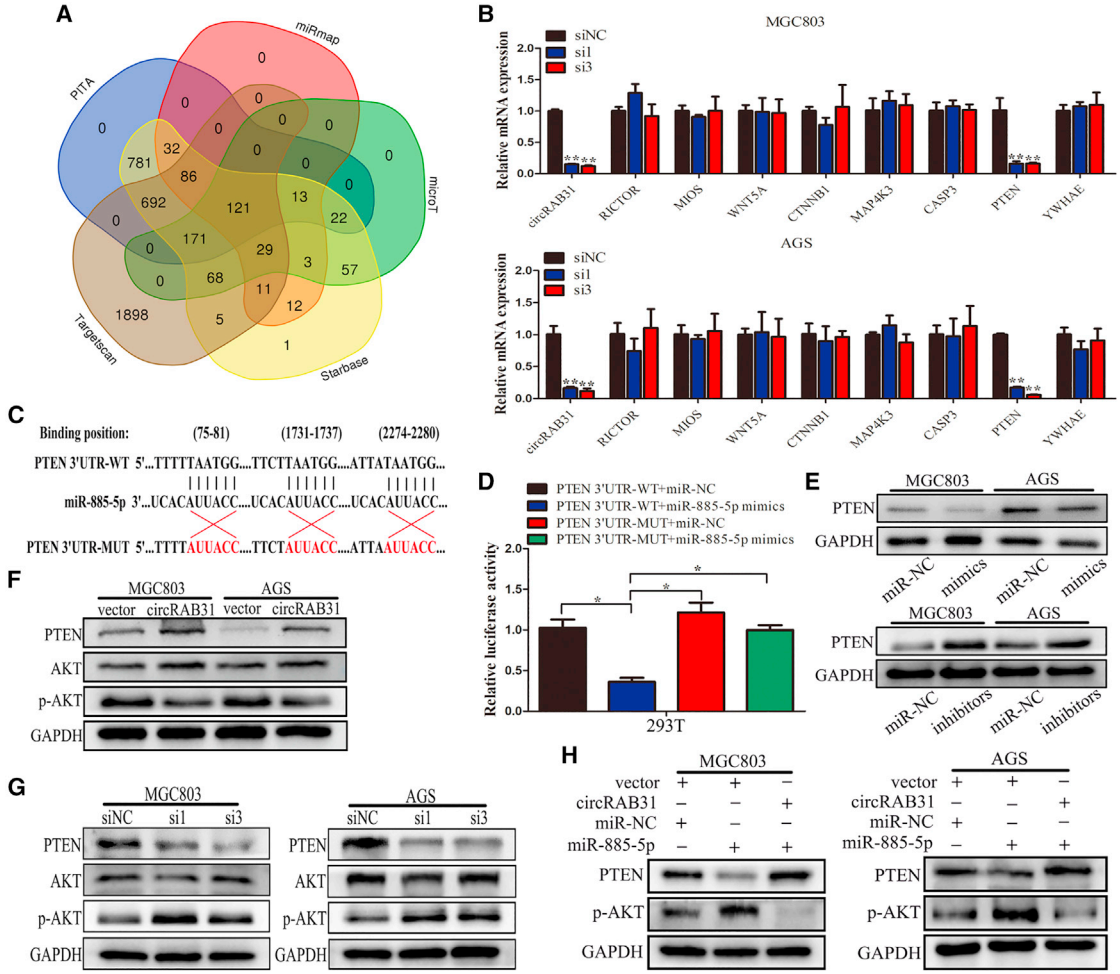

Figure 6. circRAB31-miR-885-5p-PTEN/PI3K/AKT axis is responsible for the biological function suppression of GC cells

(A) Five online databases were used to predict the target genes of miR-885-5p. (B) qRT-PCR was performed to detect the potential targets involved in GC-related signaling pathways (**p < 0.01). (C) A schematic drawing exhibited that the putative binding sites of miR-885-5p with PTEN 3′ UTR. (D) Luciferase reporter assay was performed to determine the effect of miR-885-5p on PTEN 3′ UTR in 293T cells (*p < 0.05). (E) Western blot was performed to evaluate the effect of miR-885-5p mimics and inhibitors on PTEN protein expression in MGC803 and AGS cells. (F and G) Western blot was used to detect the protein level of PTEN, AKT, and p-AKT in MGC803 and AGS cells after transfection of circRAB31. (H) Western blot analysis of the expression of PTEN and p-AKT after the co-transfection of circRAB31 and miR-885-5p mimics in MGC803 and AGS cells.

circRAB31 inhibits GC cell malignant behaviors by upregulating PTEN

Next, we explored how the circRAB31/miR-885-5p axis affected GC biological processes. Bioinformatics analysis (miRmap, PITA, Targetscan, Starbase, and microT databases) revealed 121 potential downstream genes of miR-885-5p (Figure 6A). Among these genes, we selected those involved in the most significant signaling reported to be responsible for GC progression including WNT, mTOR, and MAPK, as well as the PI3K pathways, and evaluated the effects of circRAB31 knockdown on these potential downstream targets by detecting their mRNA expression levels (WNT5A, CTNNB1 for WNT signaling; RICTOR and MIOS for mTOR signaling; MAP4K3 and CASP3 for MAPK signaling; PTEN and YWHAE for PI3K/AKT signaling). We found that circRAB31 silencing strikingly decreased mRNA expression of PTEN, implying that the circRAB31/miR-885-5p axis might regulate PTEN mRNA expression (Figure 6B). To further validate whether the circRAB31/miR-885-5p axis directly regulated PTEN, we cloned WT and MUT 3′ UTR of the PTEN into the luciferase vector and conducted the luciferase reporter assay (Figure 6C). Then, we performed dual-luciferase reporter assay and observed that co-transfection of WT 3′ UTR of the PTEN and miR-885-5p mimics resulted in a significant reduction in luciferase reporter activity relative to co-transfection with miR-NC. However, co-transfection of MUT 3′ UTR of the PTEN with miR-885-5p mimics or miR-NC did not cause a significant reduction in luciferase reporter activity (Figures 6D and S2E). Moreover, qRT-PCR and western blot analysis confirmed the regulatory effect of miR-885-5p on PTEN. Transfection of miR-885-5p mimics significantly inhibited PTEN expression, while miR-885-5p inhibitors increased the mRNA and protein level of PTEN (Figures 6E and S2F).

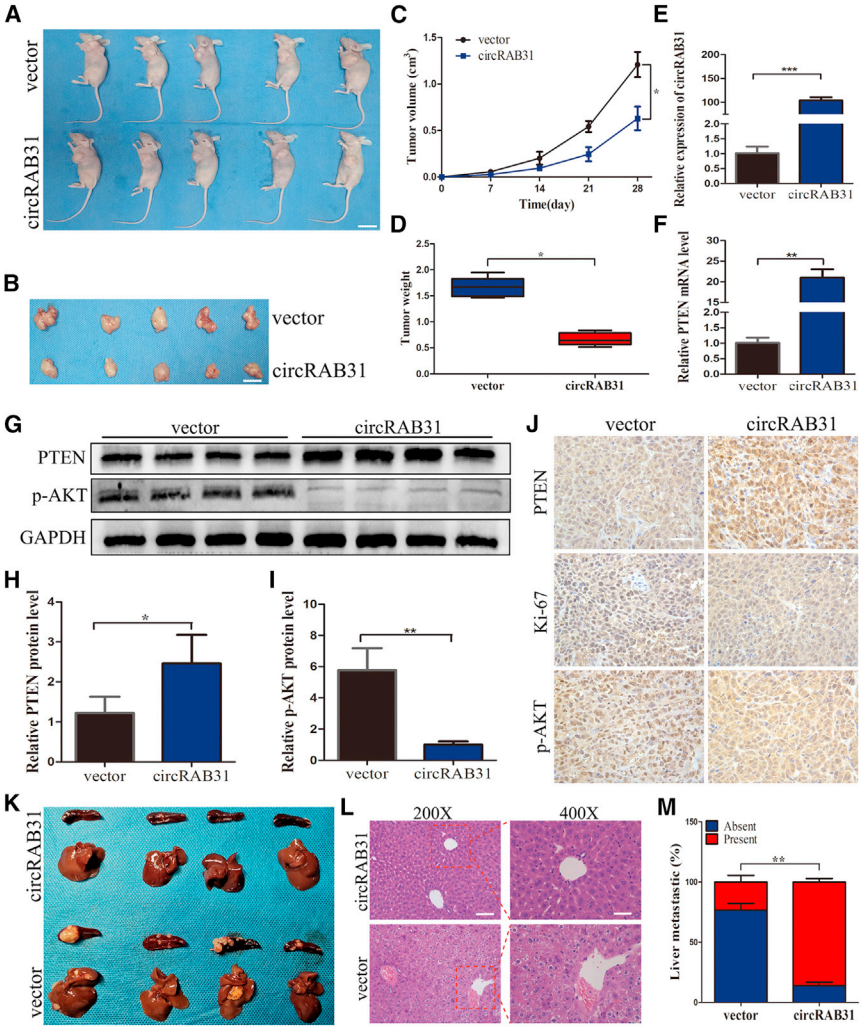

Figure 7. circRAB31 suppressed GC tumor growth and metastasis *in vivo*

(A and B) The xenograft tumors induced by circRAB31 overexpression and empty vector in MGC803 cells were exhibited; scale bar, 1 cm. (C and D) Tumor weights and tumor growth curves were analyzed (*p < 0.05). (E and F) qRT-PCR was performed to detect the mRNA expression of circRAB31 and PTEN in tumors (***p < 0.001, **p < 0.01). (G–I) Western blot assay indicated that circRAB31 could promote PTEN protein expression and inhibit p-AKT protein level (*p < 0.05, **p < 0.01). (J) IHC analysis of PTEN, Ki-67, and p-AKT obtained from tumors (magnification, ×400; scale bar, 150 μm). (K–M) Liver metastasis model revealed that circRAB31 could inhibit the metastasis ability of MGC803 cells *in vivo* (magnification, ×200, scale bar, 240 μm; magnification, ×400, scale bar, 120 μm).

These findings indicated that the circRAB31/miR-885-5p axis might regulate GC malignant behaviors by affecting PTEN expression.

circRAB31-miR-885-5p-PTEN/PI3K/AKT axis is responsible for suppressing the biological function of GC cells

PTEN, a tumor suppressor, plays a crucial role in multiple cancer types.[28–30] Loss of PTEN results in the activation of the PI3K/AKT/mTOR pathway.[31,32] To further understand the mechanism underlying PI3K/AKT signaling mediated by circRAB31/miR-885-5p/PTEN axis, we performed western blot; our results showed that circRAB31 overexpression increased PTEN protein level and decreased protein expression of p-AKT, while silencing of circRAB31 inhibited PTEN expression and promoted p-AKT expression (Figures 6F and 6G). Our findings are consistent with the previous report that PTEN inhibits the PI3K/Akt pathway by regulating the phosphorylation of Akt.[32] To determine whether miR-885-5p is responsible for the inhibition of the PI3K/Akt pathway achieved by circRAB31, we co-transfected circRAB31 with miR-885-5p mimics and determined the protein level of PTEN and p-AKT in GC cell lines. The results showed that miR-885-5p inhibited PTEN expression and promoted the protein level of p-AKT, while circRAB31 reversed the downregulation of PTEN induced by miR-885-5p and attenuated the upregulation of p-AKT caused by miR-885-5p (Figure 6H).

Taken together, we demonstrated that the circRAB31-miR-885-5p-PTEN/PI3K/AKT axis suppressed GC malignancy *in vitro*.

circRAB31 suppressed GC tumor growth and metastasis *in vivo*

To extend our *in vitro* findings and verify that circRAB31 has a tumor suppressor function *in vivo*, stable MGC803 cells overexpressed with vector or circRAB31 were injected into 4-week-old female nude mice. Tumor volume was measured using a vernier caliper every 7 days. We observed that xenograft tumors overexpressing circRAB31 grew slower compared with the control group (Figures 7A and 7B). Tumor volume and weight in the circRAB31 group were markedly lower compared with the control groups (Figures 7C and 7D). To further determine whether circRAB31 inhibits GC progression through the PTEN/PI3K/AKT axis *in vivo*, we isolated total RNA from xenograft tumors; we found that the mRNA level of PTEN in tumors with circRAB31 overexpression was higher than that in the negative control group (Figures 7E and 7F). Western blotting and immunohistochemical staining confirmed the upregulation of PTEN and the suppression of p-AKT in the circRAB31 overexpression group compared with the control group (Figures 7G–7J). Moreover, Ki-67 was determined to be downregulated in circRAB31 overexpression group relative to the control group (Figure 7J).

Next, we determined whether circRAB31 could affect the metastasis of GC cells in tumor metastasis models. Stable MGC803 cells overexpressed with vector or circRAB31were inoculated into the spleen of

female nude mice. We found that the circRAB31 overexpression group had a fewer number of metastatic nodules compared with the control group (Figures 7K–7M).

These results further confirmed the suppressive role of circRAB31 in GC via the PTEN/PI3K/AKT signaling pathway mediated by miR-885-5p.

DISCUSSION

circRNAs are a large number of conserved noncoding RNAs characterized by covalently closed-loop structures.[33] circRNAs are involved in mutiple biological processes, including tumorigenesis.[34] Mounting evidence has shown that circRNAs could function as tumor promotors or tumor suppressors in various cancers.[35–38] The roles of different types of circRNAs in GC have been preliminarily explored.[39–41] However, the mechanism by which circRNAs regulate GC progression remains largely unknown. In our study, we screened our microarray and identified circRAB31 (Has_circ_0008821) was downregulated in GC tissues compared with adjacent normal tissues. We also performed qRT-PCR and confirmed that circRAB31 was lower in tumor tissues and GC cell lines compared with adjacent normal tissues and GES-1 cells. Functionally, overexpression of circRAB31 inhibited the cellular capabilities of proliferation, migration, and invasion both *in vitro* and *in vivo*, while silencing of circRAB31 had the opposite effects. Our findings suggest that circRAB31 may play a crucial role in GC development.

RNA FISH revealed the cytoplasmic and nuclear localization of circRAB31 in MGC803 and AGS cells. Mounting evidence indicated that cytoplasmic circRNAs could function as sponges for miRNA to modulate the mRNA level of oncogenes or tumor suppressor genes.[20,24,36] We first explored whether circRAB31 could function as an miRNA sponge. Through the prediction database, we identified three potential miRNAs targeting circRAB31. RNA pull-down and luciferase reporter assay were further conducted to confirm that circRAB31 could function as a miR-885-5p sponge in GC cells. miR-885-5p has been reported to play a crucial role in various cancers, including GC.[25,27,42] To clarify the competing endogenous (ceRNA) mechanism mediated by miR-885-5p, we performed a rescue experiment and proved that circRAB31 could partially attenuate the influence of miR-885-5p mimics on GC cell proliferation, migration, and invasion. These results indicated that circRAB31 could function as a tumor suppressor gene via sponging miR-885-5p. Many previous studies also suggested that nuclear circRNAs exert crucial roles in tumor progression through interacting with proteins. circRNA FECR1 could function as a tumor promotor by recruiting TET1 to the promoter of its own host gene in breast cancer.[43] circ-DONSON was reported to promote the transcription of SOX4 through interacting with NURF complex.[44] circRAB31 was determined to localize in the nucleus of GC cells. We speculated that nucleus circRAB31 might also exert a tumor suppression role through affecting the function of Pol II or interacting with other proteins. In future studies, we will further explore the potential function of nucleus circRAB31 in GC progression.

To further identify miR-885-5p target genes mediated by circRAB31, we conducted bioinformatics analysis and identified 121 potential target genes of miR-885-5p. Then, we transfected circRAB31 siRNA and detected the mRNA expression of eight target genes involved in signaling pathways related to GC. Silencing of circRAB31 significantly decreased PTEN mRNA level in MGC803 and AGS cells. These findings indicated that PTEN might be the target gene of miR-885-5p mediated by circRAB31. A recent study also revealed that PTEN might be the target gene of miR-885-5p.[45] In particular, miR-885-5p has also been reported to modulate mRNA expression of PTEN, thereby affecting AKT/mTOR signaling in alcohol-induced osteonecrosis of the femoral head.[46] To further verify that PTEN is a direct downstream gene of miR-885-5p, we conducted luciferase reporter assay and proved that miR-885-5p could directly regulate PTEN. In addition, qRT-PCR and western blot were conducted to confirm the regulation of circRAB31 and miR-885-5p on PTEN. These results indicated that circRAB31 could function as a sponge for miR-885-5p to modulate PTEN mRNA and protein level, thereby affecting biological function of GC cells.

PTEN, one of the most frequently mutated genes, is well characterized as a crucial tumor suppressor.[47] Previous studies have reported that PTEN plays an essential role in various cancers.[28–30] PTEN also has a crucial function in the maintenance of cancer stem cells.[48,49] To identify PTEN-regulated pathways, Vivanco et al. conducted transcriptional profiling and revealed that the Jun-N-terminal Kinase pathway was activated upon PTEN loss in an AKT-independent manner.[50] In addition, two groups of authors demonstrated that the loss of PTEN resulted in the activation of the PI3K/AKT/mTOR pathway.[31,32] To clarify the underlying mechanism mediated by circRAB31/miR-885-5p/PTEN axis, we performed western blot and found that PTEN induced by circRAB31 overexpression decreased the protein level of p-AKT, while silencing of circRAB31 inhibited the PTEN protein level and promoted the p-AKT protein level. In addition, circRAB31 reversed the protein change of PTEN and p-AKT induced by miR-8855p. These results further validated the function of circRAB31 as a tumor suppressor by sponging miR-885-5p. In the final step, we validated that circRAB31 suppressed GC tumor growth and metastasis *in vivo*. Taken together, our findings demonstrated that the circRAB31-miR-885-5p-PTEN axis regulated GC cells malignance by affecting the PI3K/AKT signaling.

In conclusion, we screened our microarray to identify a downregulated circRNA circRAB31 in GC. Functional experiments indicated that circRAB31 inhibited GC cell proliferation, migration, and invasion both *in vitro* and *in vivo*. Mechanistically, circRAB31 inhibited PI3K/AKT signaling through the circRAB31-miR-885-5p-PTEN axis. Our findings suggest that circRAB31 could be a potential target for the diagnosis and treatment of GC. Understanding the circRAB31/miR-885-5p/PTEN/PI3K/AKT axis might shed light on GC development.

MATERIALS AND METHODS

Human tissue samples and cell culture

A total of 41 pairs of GC tissues and adjacent normal tissues were collected from the First Affiliated Hospital of Chongqing Medical University (Chongqing, China). Pathologic examination confirmed that the resected sample was GC tissue. This study was approved by the Ethics Committee of the First Affiliated Hospital of Chongqing Medical University.

Human embryonic kidney cell line (HEK293T), GC cell lines (AGS, MGC803, MKN45, and BGC823), and a normal human gastric epithelial cell line (GES-1) were bought from the Type Culture Collection of the Chinese Academy of Sciences (Beijing, China). These cell lines were cultured with RPMI 1640 (GIBCO, Carlsbad, CA) supplemented with 10% certified fetal bovine serum (FBS) (VivaCell, Shanghai, China).

Construction of stable cell lines and transfection

For the construction of stable overexpressing and stable knockdown of GC cell lines, we purchased lentivirus from Genechem (Shanghai, China) and infected MGC803 and AGS with lentivirus. Subsequently, 10% FBS containing 2 μg/mL puromycin (Beyotime, Shanghai, China) was used to screen stably overexpressing and stably knockdown GC cell lines.

circRAB31 siRNA, all miRNA mimic, inhibitor, and their corresponding normal control were designed and synthesized by RiboBio (RiboBio, Guangzhou, China). The detailed nucleotide sequences are listed in Table S1. WT and MUT dual-luciferase reporter plasmid of circRAB31 and 3′UTR of PTEN were bought from Gene Create (Gene Create, Wuhan, China). For transfection, Plasmid and oligonucleotide were co-transfected into the GC cell lines with Lipofectamine 2000 (Invitrogen, Carlsbad, CA).

EdU staining, CCK-8 assay, colony formation assay, flow cytometry, and TUNEL

EdU Staining Kit (RiboBio, Guangzhou, China) and Cell Counting Kit-8 (DOJNDO, Japan) were used to detect cell viability. For EdU staining, $2*10^4$ GC cells/well were seeded in 96-well plates. After 24 h, cell viability was measured and evaluated according to the manufacturer's protocol. The proportion of cells incorporating EdU was detected and imaged by a fluorescence microscope (Leica, Wetzlar, Germany). For the CCK-8 assay, the cells were seeded at a density of $2*10^3$ cells/well and maintained in 96-well plates. Next, 10 μL of CCK-8 reagent was added to each well at 0, 24, 48, and 72 h. Then the cells were incubated for 2 h at 37°C. The absorbance at 450 nm was measured by using spectrophotometer (Synergy2, BioTek, USA). For the colony formation assay, GC cells were seeded into 6-well plates at a density of $1*10^3$ cells/well and maintained in RPMI 1640 for 12 days. Then, the cells were fixed using methanol and stained with 0.1% crystal violet (Beyotime, Shanghai, China).

As for the apoptosis, flow cytometry (Chongqing Medical University, College of Life Sciences) and TUNEL (RiboBio, Guangzhou, China) assays were performed to detect the apoptosis of MGC803 and AGS cells according to the manufacturer's protocol.

Cell migration, invasion assay, and wound-healing assay

For the migration and invasion assays, GC cells ($3*10^4$ and $4*10^4$) were seeded into the top of chamber (Costar, USA) with or without Matrigel matrix (BD Biosciences, USA) in invasion and migration assays, respectively; 10% FBS medium was subsequently added into the lower chamber. After 24 h, cells were fixed with methanol and stained using 0.1% crystal violet. Images were acquired with a microscope. For wound-healing assay, we seeded stable GC cells ($6*10^5$ cells/well) into 6-well plates. After cells grew to 90% concentration, we used 200 μL plastic tips to create scratches. Cells were further cultured with RPMI 1640 containing 2% FBS for 48 h. The width of the wound was imaged by a microscope every 24 h.

FISH assay

circRAB31 probes and miR-885-5p probes were designed and synthesized by GenePharma (GenePharma, Shanghai, China). The detailed nucleotide sequences of the RNA probes are listed in Table S1. FISH kit was purchased from RiboBio (RiboBio, Guangzhou, China). U6 and 18S probes were designed and synthesized by RiboBio (lnc110101 and lnc110102; RiboBio, Guangzhou, China). The FISH experiment was performed according to the manufacturer's protocol. In short, we seeded $6*10^4$ cells on cell climbing sheets and cultured in 24-well plates. After culturing for 1 day, cells were fixed and incubated with the circRAB31 and miR-885-5p probes overnight. Then, DAPI was used to stain cell nuclei. Finally, we captured images using a ZEISS LSM800 fluorescence microscope (Carl Zeiss AG, Germany).

RNA pull-down assay

The circRAB31 specific biotin-labeled probes were bought from RiboBio. The detailed nucleotide sequence of the probe is listed in Table S1. Pull-down assay was performed according to the guidelines of the manufacturer (Thermo Fisher Scientific, Waltham, MA). In Briefly, $1*10^7$ MGC803 cells were seeded into 10-cm plates. The next day, all the cells in the plate were lysed to obtain cell lysates. The biotin-labeled probes were combined with streptavidin magnetic beads at room temperature for 30 min. We subsequently incubated the cell lysates with streptavidin magnetic beads at 4°C for an hour. After washing the streptavidin magnetic beads, RNA was extracted using TRIzol (Takara, Japan) and used for further analysis.

RNA isolation and quantitative real-time PCR

Total RNA was isolated from tissues and cells using TRIzol reagent following the manufacturer's protocol (Takara, Japan). For RNase assay, 3 μg of total RNA from GC cells was incubated with or without RNase R (Epicentre Technologies, USA) for 30 min at 37°C. Cytoplasm and nuclear RNA of MGC803 or AGS cells were extracted by using the NGB-21000 Cytoplasmic & Nuclear RNA Purification Kit (Norgen, USA) following the manufacturer's protocol. For qRT-PCR assay, we synthesized cDNA using PrimeScript RT Reagent Kit (#RR037A; Takara, Japan) or miRNA reverse transcription PCR kit (RiboBio). Results were normalized using GAPDH or U6 control.

The divergent primer for circRAB31 was designed by Geneseed (Guangzhou, China). U6 forward primer was obtained from RiboBio (miRNA00002-1-100). Other forward miRNA primers were designed and synthesized by RiboBio. Reverse primer of miRNA was contained in the miRNA reverse kit (miRACM001-22; RiboBio). All mRNA primers were designed and synthesized by Sangon Biotech (Sangon Biotech, Shanghai, China). Information about primers is shown in Table S2.

Protein extracting and western blot

Cellular and tissue proteins were isolated with RIPA cell lysis buffer (Beyotime, Shanghai, China). Phosphatase inhibitors were added into the protein lysis (Beyotime). For the western blot assay, we added the proteins to SDS-PAGE. Then, proteins were transferred to a PVDF membrane (Millipore, USA). The PVDF membrane was subsequently blocked with 5% skim milk or 5% BSA (Beyotime) for 2 h at 24°C. After the membrane was blocked, we incubated it with corresponding primary antibody: anti-GAPDH (1:6,000; Proteintech, Wuhan, China), anti-PTEN (1:2,000; Proteintech, USA), anti-AKT (1:2000; Cell Signaling Technology, Boston, MA) and anti-pAKT (1:3,000, Cell Signaling Technology) at 4°C for 12 h. Next, the membrane was incubated with TBST containing corresponding second antibody (Proteintech, Wuhan, China) for 2 h. Finally, the membrane was visualized by an enhanced chemiluminescence solution ECL (Advansta, CA).

Dual-luciferase reporter gene assay

The WT and MUT plasmids of circRAB31 and PTEN 3′UTR were synthesized by Gene Create (Gene Create, Wuhan, China). After the HEK293T and MGC803 cells were seeded into 96-well plates and grown to 80% concentration, the luciferase reporter plasmid and miR-885-5p mimics or normal controls were co-transfected into HEK293T and MGC803 cells by using Lipofectamine 2000 (Invitrogen). After 48 h, the luciferase activities were measured using dual-luciferase assay kit (Beyotime) following the manufacturer's protocol.

IHC study

Tissues were fixed with 10% paraformaldehyde, and then embedded in paraffin. Tissue sections were produced for subsequent experiments. IHC staining was performed as previously described. Sections were incubated using the following antibodies: anti-PTEN (1:400; Proteintech, Wuhan, China), anti-Ki-67 (1:400; Cell Signaling Technology), anti-pAKT (Cell Signaling Technology). Images were obtained using a Leica inverted microscope (Leica, Wetzlar, Germany).

Animal studies

Eighteen female 4-week-old BALB/c nude mice were bought from the National Laboratory Animal Center (Shanghai, China). For the xenograft model, we injected stably overexpressed MGC803 and control cells ($8*10^6$ cells) into each flank of the nude mice (five mice/group). Tumor size was measured every 7 days. After 28 days, tumors were obtained for extracting RNA and proteins. For the metastasis model, we injected stably overexpressed MGC803 and control cells ($2*10^6$ cells) into the spleen of the nude mice. After 30 days, the spleen and the liver were dissected from the nude mice. Numbers of the metastatic nodules were captured with a Leica inverted microscope. Animal studies were approved by the Animal Ethics Committee of Chongqing Medical University. All experiments conformed to all relevant regulatory standards.

Statistical analysis

All statistics were analyzed by SPSS 19.0 (SPSS, Chicago, IL) and GraphPad Prism 5.0 (GraphPad Software, La Jolla, CA). The differences were analyzed using two-tailed Student's t test, χ^2 test, or ANOVA. Pearson correlation analysis was used to detected the relationship between circRAB31 and miR-885-5p. Kaplan-Meier analysis was used to determine the survival difference. The difference with $^*p < 0.05$, $^{**}p < 0.01$, or $^{***}p < 0.001$ was considered statistically significant.

ETHICS STATEMENT

This study was approved by the Ethics Committee of the First Affiliated Hospital of Chongqing Medical University. Animal studies were approved by the Animal Ethics Committee of Chongqing Medical University. All experiments conform to all relevant regulatory standards.

SUPPLEMENTAL INFORMATION

Supplemental information can be found online at https://doi.org/10.1016/j.omto.2021.11.002.

ACKNOWLEDGMENTS

This work was supported by the National Natural Science Foundation of China (81974385). We thank Prof. Fanghui Lu and Liangjun Qiao for their assistance in this manuscript.

AUTHOR CONTRIBUTIONS

L.X.L. and Q.C. designed this study and drafted the manuscript; L.X.L. and G.X. performed the cell experiment. L.X.L., Y.G.F., and Z.H. performed the animal study. C.A.Q. and Q.C. collected tissue samples and performed the statistical analysis. W.Z.W. supervised the study and revised the manuscript. All authors read and gave final approval of the manuscript.

DECLARATION OF INTEREST

The authors declare no competing interests.

REFERENCES

1. Van Cutsem, E., Sagaert, X., Topal, B., Haustermans, K., and Prenen, H. (2016). Gastric cancer. Lancet *388*, 2654–2664.
2. Sung, H., Ferlay, J., Siegel, R.L., Laversanne, M., Soerjomataram, I., Jemal, A., and Bray, F. (2021). Global cancer statistics 2020: GLOBOCAN estimates of incidence and mortality worldwide for 36 cancers in 185 countries. CA Cancer J. Clin. *71*, 209–249.
3. Chen, W., Zheng, R., Baade, P.D., Zhang, S., Zeng, H., Bray, F., Jemal, A., Yu, X.Q., and He, J. (2016). Cancer statistics in China, 2015. CA Cancer J. Clin. *66*, 115–132.
4. Nagini, S. (2012). Carcinoma of the stomach: a review of epidemiology, pathogenesis, molecular genetics and chemoprevention. World J. Gastrointest. Oncol. *4*, 156–169.

5. Jung, G., Hernández-Illán, E., Moreira, L., Balaguer, F., and Goel, A. (2020). Epigenetics of colorectal cancer: biomarker and therapeutic potential. Nat. Rev. Gastroenterol. Hepatol. *17*, 111–130.

6. Grady, W.M., Yu, M., and Markowitz, S.D. (2021). Epigenetic alterations in the gastrointestinal tract: current and emerging use for biomarkers of cancer. Gastroenterology *160*, 690–709.

7. Cocquerelle, C., Mascrez, B., Hétuin, D., and Bailleul, B. (1993). Mis-splicing yields circular RNA molecules. FASEB J. *7*, 155–160.

8. Lasda, E., and Parker, R. (2014). Circular RNAs: diversity of form and function. RNA *20*, 1829–1842.

9. Kristensen, L.S., Andersen, M.S., Stagsted, L.V.W., Ebbesen, K.K., Hansen, T.B., and Kjems, J. (2019). The biogenesis, biology and characterization of circular RNAs. Nat. Rev. Genet. *20*, 675–691.

10. Sun, X., Zhang, X., Zhai, H., Zhang, D., and Ma, S. (2019). A circular RNA derived from COL6A3 functions as a ceRNA in gastric cancer development. Biochem. Biophys. Res. Commun. *515*, 16–23.

11. Wang, L., Long, H., Zheng, Q., Bo, X., Xiao, X., and Li, B. (2019). Circular RNA circRHOT1 promotes hepatocellular carcinoma progression by initiation of NR2F6 expression. Mol. Cancer *18*, 119.

12. Xia, X., Li, X., Li, F., Wu, X., Zhang, M., Zhou, H., Huang, N., Yang, X., Xiao, F., Liu, D., et al. (2019). A novel tumor suppressor protein encoded by circular AKT3 RNA inhibits glioblastoma tumorigenicity by competing with active phosphoinositide-dependent Kinase-1. Mol. Cancer *18*, 131.

13. Pamudurti, N.R., Bartok, O., Jens, M., Ashwal-Fluss, R., Stottmeister, C., Ruhe, L., Hanan, M., Wyler, E., Perez-Hernandez, D., Ramberger, E., et al. (2017). Translation of CircRNAs. Mol. Cell *66*, 9–21.e27.

14. Yang, Y., Fan, X., Mao, M., Song, X., Wu, P., Zhang, Y., Jin, Y., Yang, Y., Chen, L.L., Wang, Y., et al. (2017). Extensive translation of circular RNAs driven by N(6)-methyladenosine. Cell Res. *27*, 626–641.

15. Yang, Y., Gao, X., Zhang, M., Yan, S., Sun, C., Xiao, F., Huang, N., Yang, X., Zhao, K., Zhou, H., et al. (2018). Novel role of FBXW7 circular RNA in repressing glioma tumorigenesis. J. Natl. Cancer Inst. *110*, 304–315.

16. Zhang, M., Zhao, K., Xu, X., Yang, Y., Yan, S., Wei, P., Liu, H., Xu, J., Xiao, F., Zhou, H., et al. (2018). A peptide encoded by circular form of LINC-PINT suppresses oncogenic transcriptional elongation in glioblastoma. Nat. Commun. *9*, 4475.

17. Lei, B., Tian, Z., Fan, W., and Ni, B. (2019). Circular RNA: a novel biomarker and therapeutic target for human cancers. Int. J. Med. Sci. *16*, 292–301.

18. Zhang, H.D., Jiang, L.H., Sun, D.W., Hou, J.C., and Ji, Z.L. (2018). CircRNA: a novel type of biomarker for cancer. Breast Cancer *25*, 1–7.

19. Li, Y., Zheng, Q., Bao, C., Li, S., Guo, W., Zhao, J., Chen, D., Gu, J., He, X., and Huang, S. (2015). Circular RNA is enriched and stable in exosomes: a promising biomarker for cancer diagnosis. Cell Res. *25*, 981–984.

20. Fang, J., Hong, H., Xue, X., Zhu, X., Jiang, L., Qin, M., Liang, H., and Gao, L. (2019). A novel circular RNA, circFAT1(e2), inhibits gastric cancer progression by targeting miR-548g in the cytoplasm and interacting with YBX1 in the nucleus. Cancer Lett. *442*, 222–232.

21. Cheng, J., Zhuo, H., Xu, M., Wang, L., Xu, H., Peng, J., Hou, J., Lin, L., and Cai, J. (2018). Regulatory network of circRNA-miRNA-mRNA contributes to the histological classification and disease progression in gastric cancer. J. Transl. Med. *16*, 216.

22. Guo, X., Dai, X., Liu, J., Cheng, A., Qin, C., and Wang, Z. (2020). Circular RNA circREPS2 acts as a sponge of miR-558 to suppress gastric cancer progression by regulating RUNX3/β-catenin signaling. Mol. Ther. Nucleic Acids *21*, 577–591.

23. Yu, J., Xu, Q.G., Wang, Z.G., Yang, Y., Zhang, L., Ma, J.Z., Sun, S.H., Yang, F., and Zhou, W.P. (2018). Circular RNA cSMARCA5 inhibits growth and metastasis in hepatocellular carcinoma. J. Hepatol. *68*, 1214–1227.

24. Huang, W., Yang, Y., Wu, J., Niu, Y., Yao, Y., Zhang, J., Huang, X., Liang, S., Chen, R., Chen, S., et al. (2020). Circular RNA cESRP1 sensitises small cell lung cancer cells to chemotherapy by sponging miR-93-5p to inhibit TGF-β signalling. Cell Death Differ. *27*, 1709–1727.

25. Li, S., Sun, M.Y., and Su, X. (2019). MiR-885-5p promotes gastric cancer proliferation and invasion through regulating YPEL1. Eur. Rev. Med. Pharmacol. Sci. *23*, 7913–7919.

26. Su, M., Qin, B., Liu, F., Chen, Y., and Zhang, R. (2018). miR-885-5p upregulation promotes colorectal cancer cell proliferation and migration by targeting suppressor of cytokine signaling. Oncol. Lett. *16*, 65–72.

27. Zhang, Z., Yin, J., Yang, J., Shen, W., Zhang, C., Mou, W., Luo, J., Yan, H., Sun, P., Luo, Y., et al. (2016). miR-885-5p suppresses hepatocellular carcinoma metastasis and inhibits Wnt/β-catenin signaling pathway. Oncotarget *7*, 75038–75051.

28. Ali, I.U., Schriml, L.M., and Dean, M. (1999). Mutational spectra of PTEN/MMAC1 gene: a tumor suppressor with lipid phosphatase activity. J. Natl. Cancer Inst. *91*, 1922–1932.

29. Wang, S., Gao, J., Lei, Q., Rozengurt, N., Pritchard, C., Jiao, J., Thomas, G.V., Li, G., Roy-Burman, P., Nelson, P.S., et al. (2003). Prostate-specific deletion of the murine Pten tumor suppressor gene leads to metastatic prostate cancer. Cancer Cell *4*, 209–221.

30. Trotman, L.C., Wang, X., Alimonti, A., Chen, Z., Teruya-Feldstein, J., Yang, H., Pavletich, N.P., Carver, B.S., Cordon-Cardo, C., Erdjument-Bromage, H., et al. (2007). Ubiquitination regulates PTEN nuclear import and tumor suppression. Cell *128*, 141–156.

31. Xue, M., Yao, S., Hu, M., Li, W., Hao, T., Zhou, F., Zhu, X., Lu, H., Qin, D., Yan, Q., et al. (2014). HIV-1 Nef and KSHV oncogene K1 synergistically promote angiogenesis by inducing cellular miR-718 to regulate the PTEN/AKT/mTOR signaling pathway. Nucleic Acids Res. *42*, 9862–9879.

32. Salmena, L., Carracedo, A., and Pandolfi, P.P. (2008). Tenets of PTEN tumor suppression. Cell *133*, 403–414.

33. Jeck, W.R., and Sharpless, N.E. (2014). Detecting and characterizing circular RNAs. Nat. Biotechnol. *32*, 453–461.

34. Geng, Y., Jiang, J., and Wu, C. (2018). Function and clinical significance of circRNAs in solid tumors. J. Hematol. Oncol. *11*, 98.

35. Jiang, T., Xia, Y., Lv, J., Li, B., Li, Y., Wang, S., Xuan, Z., Xie, L., Qiu, S., He, Z., et al. (2021). A novel protein encoded by circMAPK1 inhibits progression of gastric cancer by suppressing activation of MAPK signaling. Mol. Cancer *20*, 66.

36. Fan, Y., Wang, J., Jin, W., Sun, Y., Xu, Y., Wang, Y., Liang, X., and Su, D. (2021). CircNR3C2 promotes HRD1-mediated tumor-suppressive effect via sponging miR-513a-3p in triple-negative breast cancer. Mol. Cancer *20*, 25.

37. Chen, Y., Li, Z., Zhang, M., Wang, B., Ye, J., Zhang, Y., Tang, D., Ma, D., Jin, W., Li, X., et al. (2019). Circ-ASH2L promotes tumor progression by sponging miR-34a to regulate Notch1 in pancreatic ductal adenocarcinoma. J. Exp. Clin. Cancer Res. *38*, 466.

38. Wu, X., Xiao, S., Zhang, M., Yang, L., Zhong, J., Li, B., Li, F., Xia, X., Li, X., Zhou, H., et al. (2021). A novel protein encoded by circular SMO RNA is essential for Hedgehog signaling activation and glioblastoma tumorigenicity. Genome Biol. *22*, 33.

39. Ma, C., Wang, X., Yang, F., Zang, Y., Liu, J., Wang, X., Xu, X., Li, W., Jia, J., and Liu, Z. (2020). Circular RNA hsa_circ_0004872 inhibits gastric cancer progression via the miR-224/Smad4/ADAR1 successive regulatory circuit. Mol. Cancer *19*, 157.

40. Xia, Y., Lv, J., Jiang, T., Li, B., Li, Y., He, Z., Xuan, Z., Sun, G., Wang, S., Li, Z., et al. (2021). CircFAM73A promotes the cancer stem cell-like properties of gastric cancer through the miR-490-3p/HMGA2 positive feedback loop and HNRNPK-mediated β-catenin stabilization. J. Exp. Clin. Cancer Res. *40*, 103.

41. Lin, J., Liao, S., Li, E., Liu, Z., Zheng, R., Wu, X., and Zeng, W. (2020). circCYFIP2 acts as a sponge of miR-1205 and affects the expression of its target gene E2F1 to regulate gastric cancer metastasis. Mol. Ther. Nucleic Acids *21*, 121–132.

42. Afanasyeva, E.A., Mestdagh, P., Kumps, C., Vandesompele, J., Ehemann, V., Theissen, J., Fischer, M., Zapatka, M., Brors, B., Savelyeva, L., et al. (2011). MicroRNA miR-885-5p targets CDK2 and MCM5, activates p53 and inhibits proliferation and survival. Cell Death Differ. *18*, 974–984.

43. Chen, N., Zhao, G., Yan, X., Lv, Z., Yin, H., Zhang, S., Song, W., Li, X., Li, L., Du, Z., et al. (2018). A novel FLI1 exonic circular RNA promotes metastasis in breast cancer by coordinately regulating TET1 and DNMT1. Genome Biol. *19*, 218.

44. Ding, L., Zhao, Y., Dang, S., Wang, Y., Li, X., Yu, X., Li, Z., Wei, J., Liu, M., and Li, G. (2019). Circular RNA circ-DONSON facilitates gastric cancer growth and invasion via NURF complex dependent activation of transcription factor SOX4. Mol. Cancer *18*, 45.

45. Meng, X., Mei, L., Zhao, C., Chen, W., and Zhang, N. (2020). miR-885 mediated cardioprotection against hypoxia/reoxygenation-induced apoptosis in human cardiomyocytes via inhibition of PTEN and BCL2L11 and modulation of AKT/mTOR signaling. J. Cell Physiol. *235*, 8048–8057.

46. Hong, G., Han, X., He, W., Xu, J., Sun, P., Shen, Y., Wei, Q., and Chen, Z. (2019). Analysis of circulating microRNAs aberrantly expressed in alcohol-induced osteonecrosis of femoral head. Sci. Rep. *9*, 18926.

47. Song, M.S., Salmena, L., and Pandolfi, P.P. (2012). The functions and regulation of the PTEN tumour suppressor. Nat. Rev. Mol. Cell Biol. *13*, 283–296.

48. Zhang, J., Grindley, J.C., Yin, T., Jayasinghe, S., He, X.C., Ross, J.T., Haug, J.S., Rupp, D., Porter-Westpfahl, K.S., Wiedemann, L.M., et al. (2006). PTEN maintains haematopoietic stem cells and acts in lineage choice and leukaemia prevention. Nature *441*, 518–522.

49. Yilmaz, O.H., Valdez, R., Theisen, B.K., Guo, W., Ferguson, D.O., Wu, H., and Morrison, S.J. (2006). Pten dependence distinguishes haematopoietic stem cells from leukaemia-initiating cells. Nature *441*, 475–482.

50. Vivanco, I., Palaskas, N., Tran, C., Finn, S.P., Getz, G., Kennedy, N.J., Jiao, J., Rose, J., Xie, W., Loda, M., et al. (2007). Identification of the JNK signaling pathway as a functional target of the tumor suppressor PTEN. Cancer Cell *11*, 555–569.